Effect of surface treatment and nanoclay on thermal and mechanical performances of jute fabric/biopol 'green' composites

Mohammad K. Hossain, Mohammad W. Dewan, Mahesh Hosur and Shaik Jeelani

Journal of Reinforced Plastics and Composites 2011 30: 1841 originally published online 1 December 2011
DOI: 10.1177/0731684411430426

Article

JOURNAL OF REINFORCED PLASTICS & COMPOSITES

Journal of Reinforced Plastics and Composites
30(22) 1841–1856

DOI: 10.1177/0731684411430426
jrp.sagepub.com

SAGE

Effect of surface treatment and nanoclay on thermal and mechanical performances of jute fabric/biopol 'green' composites

Mohammad K. Hossain, Mohammad W. Dewan, Mahesh Hosur and Shaik Jeelani

Abstract

The effects of surface modification of jute fibers and nanoclay on jute–biopol green composites are evaluated by the thermal and interlaminar shear strength (ILSS) characterizations. Four subsequent chemical treatments including detergent washing, dewaxing, alkali treatment, and acetic acid treatment were performed to facilitate better bonding between the fiber and matrix. The scanning electron microscopy and Fourier transform infrared spectroscopy study confirmed improved fiber surfaces for better adhesion with matrix after final treatment. Enhanced thermal performance and tensile properties were obtained due to chemical treatments. Montmorillonite K10 nanoclay (2–4 wt.%) was dispersed into a biodegradable polymer, biopol, using solution intercalation technique and magnetic stirring. Nanoclay-infused biopol resulted in 7% improvement in the degree of crystallinity over the neat biopol. Jute fiber-reinforced biopol biocomposites with and without nanoclay were produced using treated and untreated jute fibers by the compression molding process. Treated jute fiber-reinforced biopol composites (TJBC) without nanoclay showed 5% and 9% increases in decomposition temperature and storage modulus, respectively, and 19% decrease in coefficient of thermal expansion compared to untreated jute fiber-reinforced biopol composites (UTJBC). The respective values were 5%, 100%, and 45% for 4% nanoclay-infused TJBC compared to UTJBC without nanoclay. ILSS evaluated by the short-beam shear tests, improved by 20% in the TJBC compared to the UTJBC. Incorporation of 4 wt.% nanoclay in TJBC further improved the ILSS by 22% compared to that of TJBC without nanoclay.

Keywords

natural fiber, biodegradable polymer, surface treatment, nanocomposites, thermal analysis

Introduction

Synthetic fibers such as carbon, glass, and aramid fibers are generally used to manufacture composite materials due to their better mechanical and thermal properties. However, they are expensive and non-biodegradable. Natural fibers are inexpensive, biodegradable, or recyclable due to reasonable cost, easy availability, and good mechanical, thermal, and electrical properties. Industrial crops grown for fiber have the potential to supply enough renewable biomass for various bio-products including composites. The scope of the possible uses of natural fibers is enormous.[1] In many applications such as secondary and tertiary structures, panels, packaging, and gardening items, the composites do not require strong mechanical properties. Natural fiber-reinforced green composites can be used as an alternative of synthetic fiber-reinforced composites in these applications[2,3] It has been observed that properties can be further improved by introducing a small amount of nanoparticles in composite materials[4]

Various research groups have worked on biodegradable polymeric materials such as bionolle,

Tuskegee University Center for Advanced Materials, Tuskegee University, 101 Chappie James Center, Tuskegee, AL, USA.

Corresponding author:
Mohammad K. Hossain, Tuskegee University Center for Advanced Materials, Tuskegee University, 101 Chappie James Center, Tuskegee, AL 36088, USA
Email: hossainm@mytu.tuskegee.edu

biopol (poly(3-hydroxybutyrate-co-3-hydroxyvalerate)) (PHBV), poly(3-hydroxybutyrate) (PHB), and polylactic acid[5] for use in natural fiber-reinforced composites. PHB and biopol can be considered as true biopolymers because they are synthesized by bacteria as macromolecules from renewable resources such as corn sugar and oil. PHBV has several advantages over the petroleum-based plastic, including (1) less energy required for production, (2) ability to reduce the green house gas emissions, and (3) less landfill waste generation. It can also be used in packaging, adhesives, and coating applications to replace petroleum-based amorphous and semi-crystalline polymers. It is known to be an environmental-friendly plastic because of its production from renewable resources and biodegradability to carbon dioxide and water.[6] The remaining biodegradable polymers are synthetic or semi-synthetic.[7] PHB and its copolymers are highly crystalline and have melting point, strength, and modulus comparable to those of isotactic polypropylene (PP).[8] The properties of PHBV can be enhanced by incorporating natural fibers and nanoparticles. Improved storage modulus of PHBV was reported due to the addition of cellulose nanowhisker (CNW). For example, the maximum storage modulus was observed to be 2100 MPa at 30°C with 5% CNW.[9] An addition of 40 wt% bamboo fibers into PHBV at 25°C resulted in 173% enhancement in storage modulus and about 300°C decomposition temperature.[10]

Among all natural fibers, jute fibers are easily available in fabric and fiber forms with good mechanical and thermal properties. Therefore, jute-based composite materials can be used in consumer goods, low-cost housing, and interior of cars, civil structures, and biomedical applications. Approximate chemical composition (in wt%) of jute fiber[11,12] is: cellulose – 71.5%; hemicellulose – 13.4%; pectin – 0.2%; lignin – 13.1%; water soluble compounds – 1.2%; fat and waxes – 0.6%. Cellulose is the main element of jute fiber, which is highly crystalline in nature and possesses considerably good thermal and mechanical properties. However, natural fibers do not efficiently adhere to non-polar matrices and have various impurities. To overcome this difficulty and remove impurities, these fibers should be chemically or physically modified.[13] Chemical modification of the fibers using dewaxing, treatment with alkali, acetylating, and grafting alter the surface properties for better interaction between fibers and matrix.[14] Chemically modified surfaces decrease moisture absorption and increase tensile strength[15,16] and wettability of fibers by matrix. Acha et al.[17] studied the effect of detergent washing and acetone washing of jute fabric on the jute polyester composites and found increased compression properties and decreased impact strength in the treated fiber-reinforced composites. Coupling agent maleic anhydride (MAH) was observed to have a significant effect on the mechanical properties of abaca, jute, and flax fiber-reinforced PP composites.[18] In one study,[19] 45% improvement in ILSS of jute fiber-reinforced PP composites with 5% MAH coupler has been obtained. It was documented that the storage modulus was improved by 22% in silane-treated jute fiber-reinforced PP composites at 60°C compared to that of untreated ones.[20]

Moisture barrier, flame resistance, thermal, and mechanical properties of polymeric composites can be improved by adding a small amount of nanoclay as filler particles. Clay is also environment-friendly, naturally abundant, and economical. The modulus of the nanocomposites increases and the strain to failure decreases due to the addition of nanoclay into polymeric composites.[21] The reinforcing effect depends largely on the degree of dispersion and morphology of silicate platelets into the polymer matrix, which in turn is a function of the polymer–nanoclay compatibility. Nanoclay should be exfoliated into the matrix to obtain maximum benefits out of it. However, a combination of exfoliated and intercalated morphologies is obtained in most of the cases. Processing techniques currently being used to disperse nanoclay into polymer matrix are exfoliation–adsorption, *in situ* polymerization, solution intercalation, and template synthesis. Nanoclay agglomerates into the composites due to the improper dispersion. A stabilization process is used to remove larger clay agglomerates in the nanoclay suspension.[9,22] A thermogravimetric analysis (TGA) study demonstrated the improved thermal stability of the PHBV due to the addition of 1–5 wt.% silica nanoparticles, indicating the effective barrier properties of nanofillers to the heat and mass transport.[6] The decomposition temperature of this polymer was also increased by about 5°C due to the incorporation of 5 wt.% SiO_2 nanoparticles. Decreasing coefficient of thermal expansion (CTE) values with increasing percentage of fiber and cellulose acetate with triethyl citrate reinforced with 30% hemp fibers was observed by one research group.[23] Addition of nanoclay also decreased the CTE of hemp fiber-reinforced modified unsaturated polyester composite.[24] It was also found that ILSS was improved by 31% in glass epoxy composites due to the addition of 2% oxidized multi-walled carbon nanotubes.[25]

There are quite limited data on the synergistic effect of jute fiber (treated and untreated) and nanoclay. The objectives of this research are twofold. The first is to study the effect of surface treatment of the fibers on the properties of the composite material. The second is to study the effect of introduction of a small amount of nanoclay on composites made from both treated and

untreated jute fibers. Jute fibers were chemically treated with a modified four-step process for better interfacial adhesion with matrix and evaluated by the scanning electron microscopy (SEM), Fourier transform infrared spectroscopy (FTIR), TGA, and tensile tests. Treated/untreated jute fiber-reinforced biopol green composites with/without nanoclay were produced using the compression molding process and characterized using TGA, thermo-mechanical analysis (TMA), dynamic mechanical analysis (DMA), and short-beam shear tests.

Experimental procedure

Materials

Polyhydroxybutyrate/polyhydroxyvalerate 12%-Biopolymer-Granule (PHB88/PHV12) obtained from Goodfellow Cambridge Ltd. (UK) (grade: PHB88/PHV12, trade name: biopol, average molecular weight = 90,3000 g/mol, and melt flow index (ASTM 1238-906) 190°C (2.16 kg load): 8^{26}), hessian jute fabrics (Natural Color Burlap, Material: 100% Jute, plain weave, and surface weight = 0.373 kg/m^2) supplied by OnlineFabricStore.net, and montmorillonite K10 nanoclay (organoclay, cationic exchange with alkyl ammonium salt cationic surfactants, and surface area-= 220–270 m^2/g) procured from Sigma–Aldrich (USA) were used as matrix, reinforcement, and nanofillers, respectively. Alcojet detergent, 50% ethanol solution, 50% NaOH solution, and 99% acetic acid solution for chemical treatments, and 99% chloroform solution to dissolve biopol were used.

Surface modification of jute fiber

Detergent washing, dewaxing, alkali treatment, and soaking with acetic acid were performed on hydrophilic jute fibers to improve interfacial bonding with biopol which is a hydrophobic polymer. Dirt was removed from fibers by detergent washing. Fibers were immersed in 5% detergent solution at 30°C for 1 h and subsequently washed with water and dried. Pectin was removed from these dried fibers by immersing them into 5% ethanol solution at 30°C for 1 h. This was followed by washing with water and drying. Dewaxed fibers were kept into 5% NaOH solution at 30°C for different time periods (1–5 h). The alkali-treated fibers were then washed several times with distilled water to remove lignin, hemicelluloses, and excess alkali from the fiber surface. The final pH was maintained at 7.0. Though the hemicellulose and lignin of fiber leach out due to alkali treatment, the cellulose content remains unaffected before and after alkali treatment of the fiber.[27] The alkali treatment also breaks the hydrogen bonding between the hydroxyl groups (–OH) of the cellulose, hemicellulose, and lignin in fiber and leads to defibrillation, i.e., breaking down the fiber bundle into single fibers. The reaction of NaOH with cellulose is given below:[28]

$$\text{Cellulose} - \text{OH} + \text{NaOH} \rightarrow \text{Cellulose} - \text{O} - \text{Na} + + \text{H}_2\text{O}$$

Thus, alkali treatment increases the effective surface area available for interacting with the matrix, and alkali-treated fibers treated for 2 h showed optimum results reported by the authors elsewhere.[29]

Alkali treatment resulted in a large number of –OH group accessible on the surfaces of fibers.[30] Alkali-treated fibers were soaked with distilled water–acetic acid (2%) solution for 1 h, followed by washing with distilled water and drying. Acetic acid efficiently removes the sodium ions that were deposited on fibers during alkali treatment. Some traces of the acid are also reacted with −OH group on fiber surfaces, which is important for better adhesion with biopol. Before and after surface modification, the physical appearances of the jute fibers were analyzed using digital photographs and optical micrographs (Figure 1). Untreated fibers contained dirt and the micrographs are observed to be dark. Surface treatments resulted in the removal of impurities; thus, the micrographs look clean and shiny.

Composite fabrication

Jute–biopol composites were fabricated using treated and untreated fibers and biopol by the compression molding process. Biopol was dissolved into chloroform at a ratio of 1:8 at room temperature and stirred by magnetic stirrer for 4 h to prepare a homogeneous solution. In the case of nanophased composites, nanoclay was infused into biopol using the solution intercalation technique.[31] The nanoclay was mixed with chloroform using magnetic stirring and the solution was then mixed with the biopol chloroform solution and stirred for 2 h to prepare a homogeneous mixture. This mixture was then poured into a mold to prepare a 1.5-mm thick film and dried in a vacuum oven at 60°C to evaporate choloroform. Next, dried films were placed in the hot press and 13.34 kN force was applied at 166°C for 10 min to prepare 0.50 mm thin films. Jute–biopol composites were produced by stacking films and fibers like a sandwich using the compression molding process applying 13.34 kN force at 166°C for 15 min.

The fiber volume of the fabricated composites was calculated using the composite mixing rule formula documented elsewhere by the authors.[29] To calculate the fiber volume fraction, the weight fractions of fiber, matrix, and nanoparticles were determined by measuring the individual weight of each component

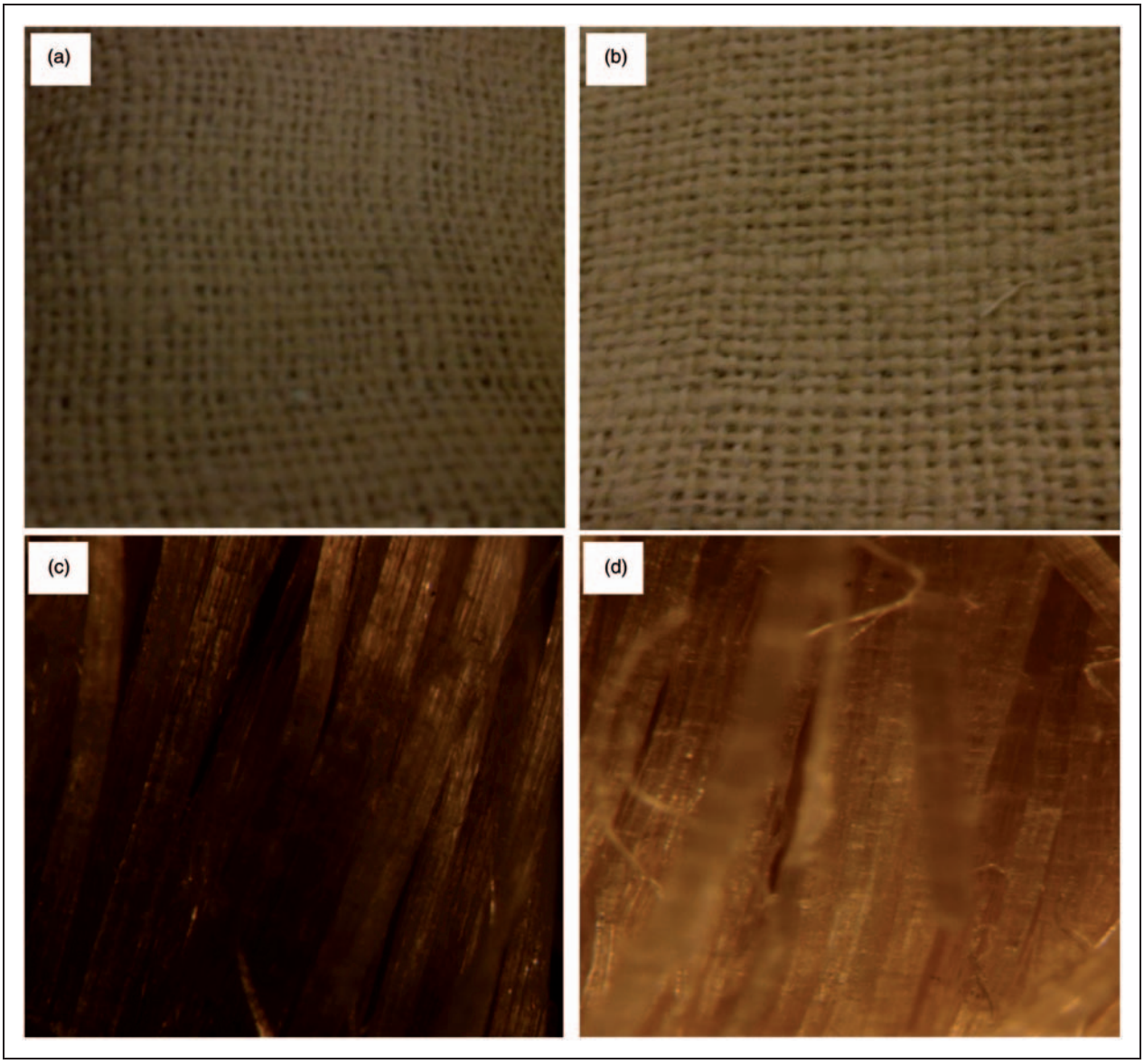

Figure 1. Digital photographs of: (a) untreated and (b) treated jute fibers. Optical micrographs of: (c) untreated and (d) treated jute fibers.

during fabrication. Using weight fraction and density of the individual constituents, the fiber volume fraction was calculated.

Fiber characterization procedures

The FTIR spectra of parent and surface-treated fibers were recorded using Nicolet 6700 DX IR spectrophotometer with attenuated total reflectance (ATR) sampling. The crystal material used for the ATR was diamond. The background was taken after every 60 min and each spectrum recorded by co-adding 32 scans at 4 cm^{-1} resolution within the range 4000–600 cm^{-1}. FTIR spectra technique was used to find the functional groups present both above and just below the top molecular layer of flat surface.[32] The spectra for each of the samples were reproducible for different samplings of these materials, indicating that the samples were homogeneous.

Tensile properties of untreated and treated jute fiber bundles were characterized using a Zwick–Roell testing unit according to the ASTM D2256-02 standard under displacement control mode on a gauge length of 50 mm at a strain rate of 0.5 min^{-1}. Young's modulus was calculated in the elastic region (0–2% strain) of the stress–strain curve.

Morphological characterization of the treated and untreated jute fibers was conducted using a JEOL

JSM-5800 SEM. Fibers were coated with silver to prevent charging. An accelerating voltage of 5 kV was used to collect the SEM micrographs. All micrographs were taken at the same voltage and magnification.

TGA was conducted with a TA Instruments Q 500 setup fitted with nitrogen purge gas in order to acquire information about thermal stability of the jute fibers, biopol, and jute–biopol composites. Samples were kept in a platinum sample pan, weighed, and heated to 450°C from room temperature at a heating rate of 10°C/min under nitrogen atmosphere. The real-time characteristic curves were generated by a Universal Analysis-TA Instruments, Inc. data acquisition system.

Matrix characterization procedures

Differential scanning calorimetry (DSC) experiments were carried out using a TA Instruments Q 1000 setup with sealed aluminum pans at temperatures ranging from room temperature to 200°C at a heating and cooling rate of 5°C/min under nitrogen atmosphere. The melting and cold crystallization temperatures (T_m and T_{cc}, respectively) of biopol and nanoclay-infused biopol were determined from the heating cycle. Crystallization temperature (T_c) was determined form the cooling curve. The degree of crystallinity was measured using the following equation: $X_c = [H_m/(1 - \emptyset) \times H_0]$, where H_m is the enthalpy of melting, $\emptyset$ the weight fraction of nanofiller, and H_0 the melting enthalpy of pure (100% crystalline) biopol (115 J/g).[33]

Composite characterization procedures

TMA tests were performed with TA instruments Q 400 setup operating in the penetration mode at a heating rate of 5°C/min from room temperature to 120°C under nitrogen gas atmosphere to find the CTE value of the jute–biopol composites.

Storage modulus (the dynamic elastic response of the sample), loss modulus (the dynamic plastic response of sample), tan δ (the ratio of loss modulus (E'') and storage modulus (E')), and storage modulus (E') of jute–biopol composite samples were obtained from DMA. The tests were carried out using a TA Instruments Q 800 setup under three-point bending mode at a heating rate of 5°C/min from 30°C to 120°C with an oscillation frequency of 1 Hz and an amplitude of 15 μm according to the ASTM D4065-01 standard.[34] Nominal specimen dimensions were $60 \times 12 \times 3\,mm^3$.

ILSS testing was carried out using a Zwick–Roell testing unit under three-point bending mode according to the ASTM D 2344-84 standard at a cross-head speed of 1.3 mm/min. Span length-to-depth ratio was 5 and the width was 6.5 mm. Using a short beam, it is assumed that the beam is short enough to minimize bending stresses, resulting in an interlaminar shear failure by cracking along a horizontal plane between the laminae. The force applied at the time of failure was recorded and the ILSS was calculated using the equation $ILSS = (0.75 \times P_b)/(b \times h)$, where P_b is the breaking load (N), and b and h are the width and thickness of the specimen in millimeters, respectively. Three identical specimens from each category were tested and the average ILSS was calculated.

Fracture morphology of the tested specimens was studied by Olympus DP72 optical microscope (OM) and its magnification varied from 7× to 115×.

Results and discussions

Fiber characterization

Figure 2 illustrates the FTIR spectra of modified jute fibers. A broad absorption band in the region 3200–3600 cm^{-1}, characteristic of hydrogen-bonded O–H stretching vibration,[35] was common to all the spectra. The alkali treatment causes the intensity of this peak to decrease due to the reduction of intermolecular/intramolecular hydrogen bonding between the hydroxyl groups of cellulose and hemicelluloses of fiber. On the other hand, the alkali (NaOH) treatment resulted in more O–H groups which become accessible on the fiber surface[30] for the reaction with the acetyl group of the acetic acid. The hydroxyl group is also present in hemicelluloses and pectin. Surface treatment resulted in the removal of some percentage of hemicelluloses and pectin. Thus, the O–H stretching vibration peak was decreased due to surface treatments. The C–H stretching vibrations of methyl and methylene groups in cellulose and hemicellulose were observed near wave number 2950 cm^{-1}.[24] They also decreased due to the surface modification. Hemicellulose was the main concern of our surface modification, which appeared near the wave number 1730 cm^{-1} for the C = O stretching vibration of the carboxylic acid and ester components of hemicellulose. This peak is also responsible for lignin. Hemicellulose and lignin were dissolved into the alkali solution and no peaks were observed in the alkali-treated fibers for C = O stretching vibration. The absorbance of a band at 1464 cm^{-1} is assigned for $-CH_3$ and 1376 cm^{-1} assigned for C–H stretching vibration of lignin.[36] These peaks were weakened due to the chemical treatment, which is an indication of removal of lignin from the treated fibers. The characteristic peak at 1430 cm^{-1} is for $-CH_2$ bending of cellulose, which remains almost unaffected in the 2-h alkali-treated fibers.[37] The peak at 1249 cm^{-1} associated to C–O stretching in the acetyl groups in hemicelluloses[38] is also weakened for the surface treatment,

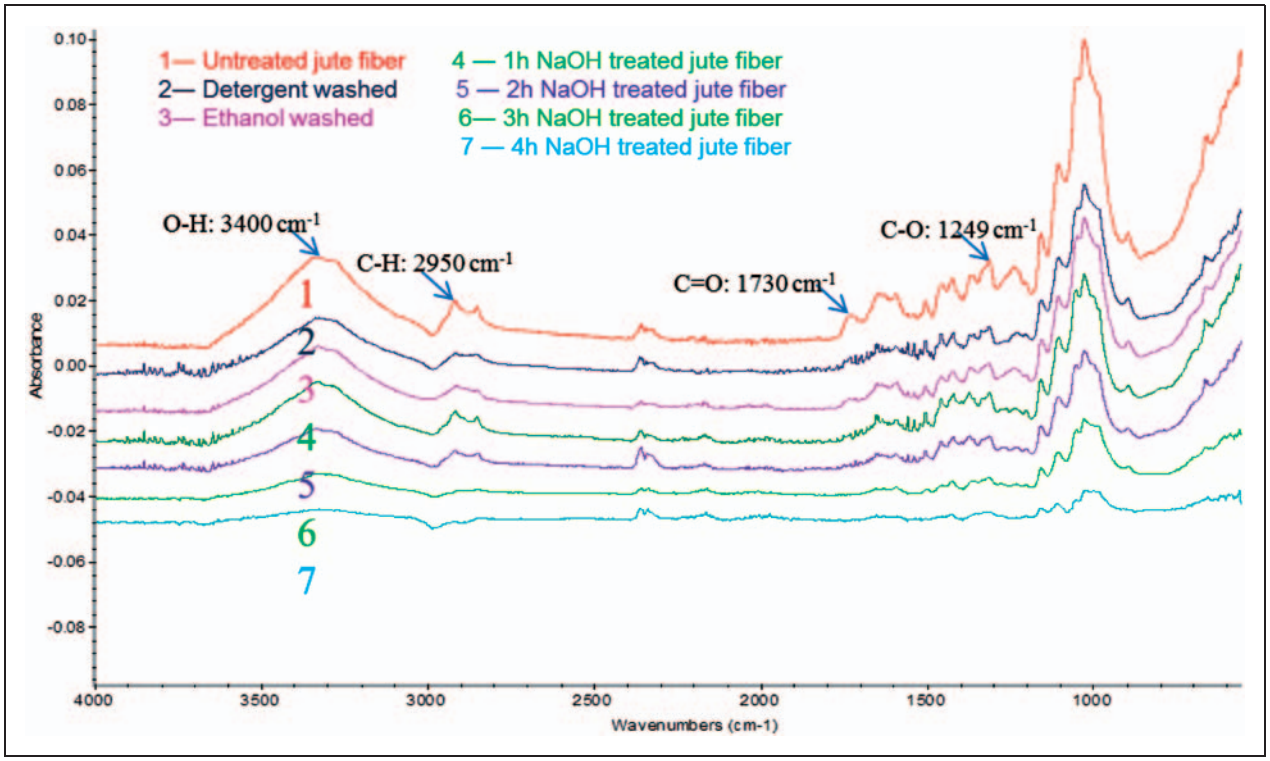

Figure 2. FTIR spectra of treated and untreated jute fibers.

Table 1. Tensile test results of treated and untreated jute fibers

Jute fiber bundle	Strength (MPa)	Strength change (%)	Strain at failure (%)	Strain change (%)	Modulus (GPa)	Modulus change (%)
Untreated	81.42 ± 10.00	0	3.83 ± 0.62	0	1.92 ± 0.45	0
1 h NaOH treated	85.04 ± 13.00	4.9	3.62 ± 0.67	−5	2.06 ± 0.64	7.3
2 h NaOH treated	92.54 ± 11.00	13.0	3.21 ± 0.68	−16	2.25 ± 0.26	17.0
3 h NaOH treated	91.68 ± 10.00	12.0	3.34 ± 0.64	−13	2.26 ± 0.34	17.7
5 h NaOH treated	80.00 ± 13.00	−1.2	2.98 ± 0.69	−22	2.28 ± 0.74	18.7

indicating hemicellulose removal. As the exposure time of fibers into the sodium hydroxide solution increases, the percentage of cellulose content increases. About 14% weight loss was observed in finally treated jute fabrics for the removal of moisture, hemicellulose, and pectin.

Uniaxial tensile test results of treated and untreated jute fiber bundles are given in Table 1. Fibers treated with NaOH for 2 h exhibited improvements in tensile strength and modulus by 13% and 17%, respectively, compared to untreated fibers. Alkali treatment caused removal of non-cellulosic materials including hemicellulose, lignin, and pectin from interfibriller regions[20] and resulted in a higher percentage of cellulose, which was the main contributor to higher tensile strength and modulus of fibers.[36] Higher concentrations of NaOH or longer exposure to NaOH weaken fibers and make it more brittle. The 2-h treatment with 5% NaOH showed optimum results.

Surfaces of treated and untreated fibers were investigated using SEM micrographs (Figure 3). These micrographs revealed relatively rougher surfaces in treated fibers compared to untreated fibers. Removal of surface impurities, non-cellulosic substances, inorganic materials, and waxes resulted in cleaner and rougher surfaces in finally treated fibers. A mesh-like structure was observed in untreated fibers, which entangled the fibrils. Chemical treatments broke mesh-structure and caused defibrillation of fibers that provided higher strength to fibers. This observation was reported elsewhere.[39] Rougher surface and defibrillation were also attributed to a better interaction of fibers with matrix due to availability of larger effective surface area.

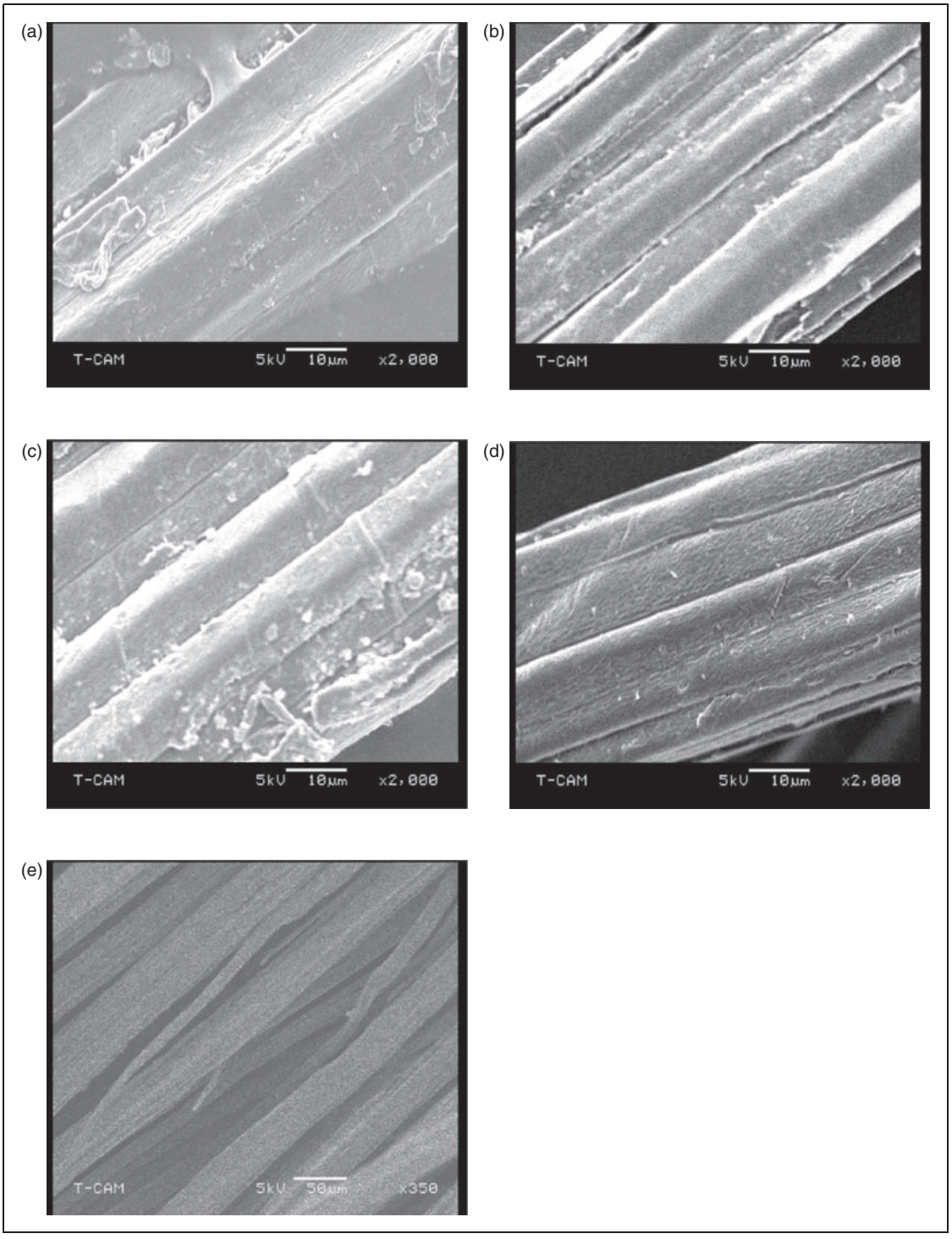

Figure 3. SEM micrographs of different stage surface-treated jute fibers. (a) Untreated jute fiber (b) Detergent washed jute fiber (c) Ethanol washed jute fiber (d) Final treated jute fiber (e) Final treated juite fiber(defibillated).

The TGA curves (Figure 4) indicate the weight loss of jute fibers and biopol. Lignocellulosic fibers contain moisture. It is evident from the figure that initially, a small amount of weight loses was observed over a wide range of temperature. This weight loss stage is due to the vaporization of the moisture present in the fibers. Chemically treated fibers had less amount of moisture (4 wt%), which is promising for jute–biopol composites. The second decomposition stage was due to the degradation of cellulosic substances. The third stage

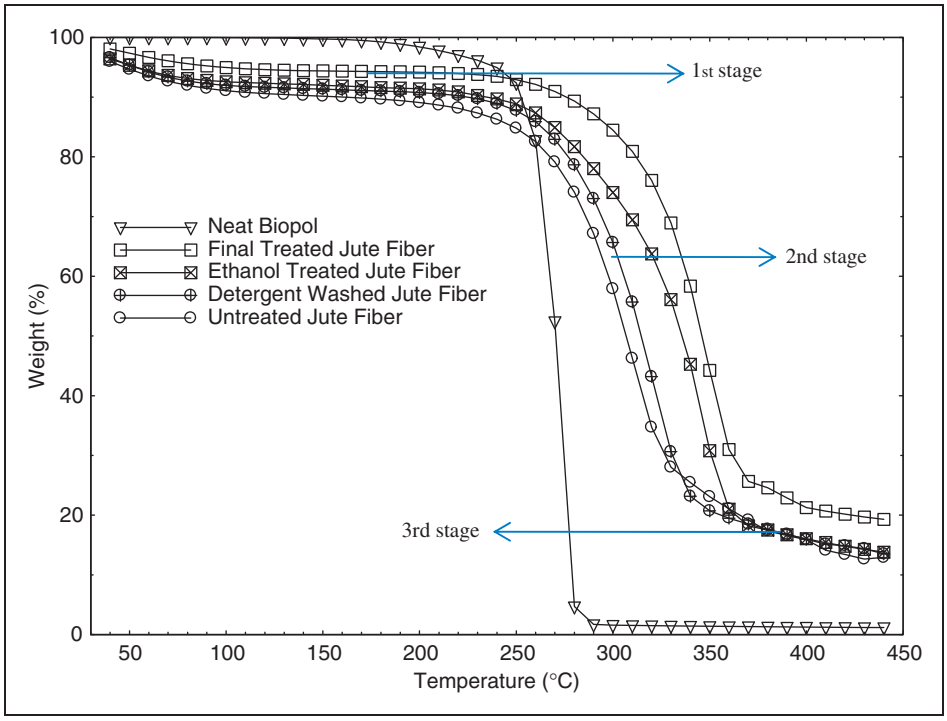

Figure 4. Percentage weight loss of jute fibers and biopol with temperature.

(after degradation temperature) was attributed to the degradation of non-cellulosic substances such as lignin and pectin.[40,41] Chemically treated fibers showed a higher decomposition temperature due to the removal of impurities, waxes, and hemicellulose by chemical treatments. Cellulose contributes to the higher thermal stability compared to other elements of lignocellulosic fibers. Thus, it can be concluded that treated fibers contain higher percentage of cellulose. When the fiber is soaked in strong caustic solution, various Na-cellulose complexes are formed,[42] which degrade the mechanical properties of jute fibers. Figure 4 shows that fibers treated with 5% alkali solution for 2 h have the highest decomposition temperature compared to other samples. Biopol starts to degrade at about 250°C, whereas fibers start to degrade around 330°C. However, sodium hydroxide has a direct effect on the mechanical properties of the fibers. Fibers exposed into the 5% sodium hydroxide solution for 2 h and washed with the 2% acidic acid solution for 1 h showed optimum results for the surface modification.

Matrix characterization

DSC curves are illustrated in Figure 5 for biopol with/without nanoclay. Incorporation of nanoclay decreased the crystallization temperature, indicating an enhanced crystallization ability of PHBV. Nanoclay acted as a nucleating agent[31] and induced PHBV crystallization at a lower temperature. Neat, 2%, 3%, and 4% nanoclay-infused biopols showed 44.36%, 47.46%, 47.47%, and 47.67% degrees of crystallinity, respectively. Samples with nanoclay showed improvement by 7% in the degree of crystallinity compared to samples without nanoclay (Table 2).

The bimodal endothermic peaks observed during the heating cycle are due to the crystallization phenomena of heterogeneous crystal morphology formed during processing. The slow DSC heating scans provided sufficient time for less perfect crystals to melt and reorganize into crystals with higher structural perfection. The re-organized crystals are then subsequently re-melted at a higher temperature.[43] There were two peaks present for all samples: one near 145°C and another one near 155°C, showing lower peaks for the nanoclay-loaded samples compared to the sample without nanoclay. That means that after infusing nanoclay, the number of defective crystals decreases, which is also evident from the degree of crystallinity. Therefore, the lower melting temperature peaks are attributed to the melting of imperfect crystals formed during the isothermal crystallization process. On the other hand, the higher melting temperature was found to be independent of the isothermal crystallization temperature. From the DSC results, it can be hypothesized that nanoclays affected the crystallization in two opposite ways: (1) a small portion of clays can affect the nucleation that increased the crystalline nuclei. Thus, nucleation of nanoclays resulted in a more rapid crystallization rate with more perfect crystallization structure. (2) due to

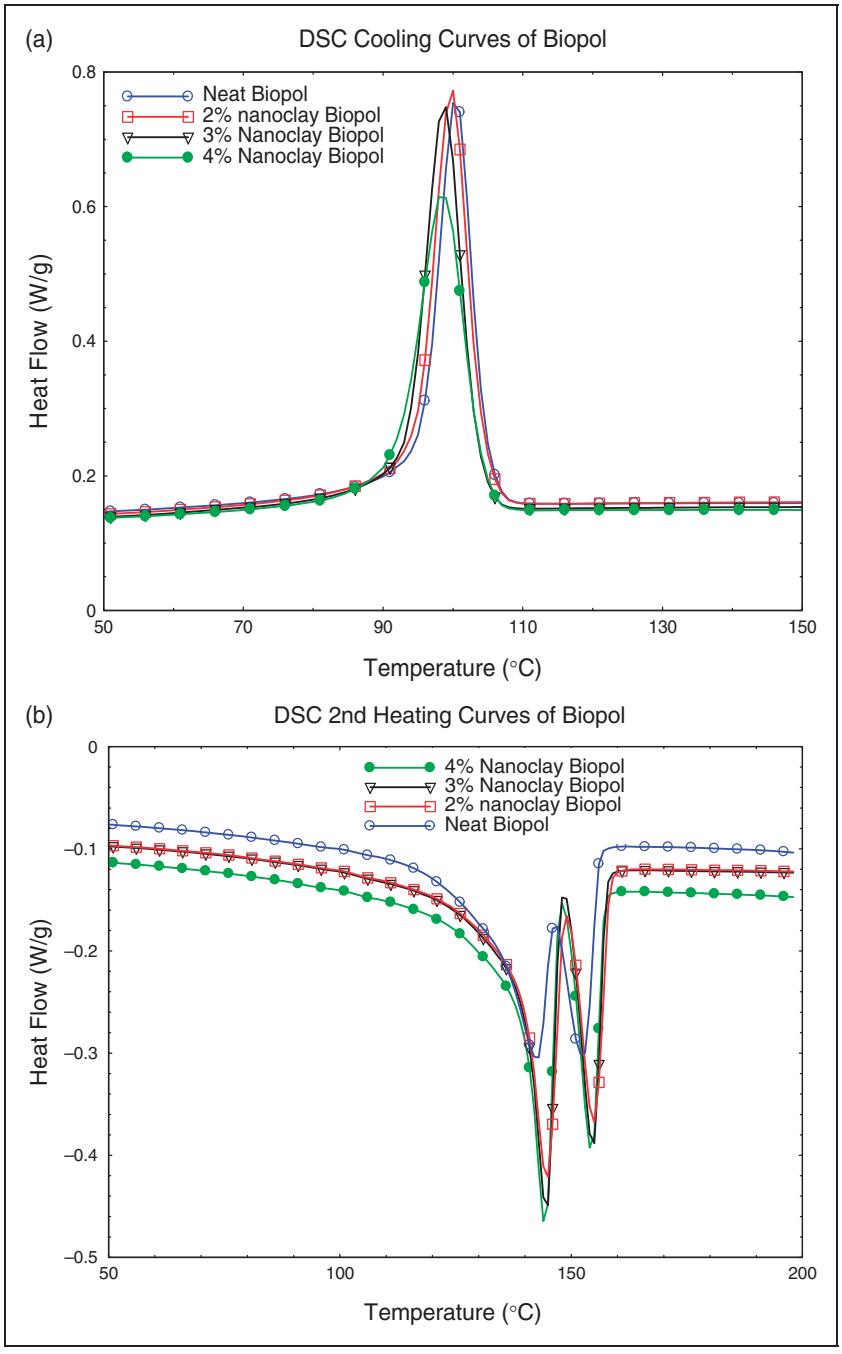

Figure 5. DSC: (a) cooling curves and (b) heating curves of neat and nanoclay-infused biopol.

Table 2. Crystallization temperature and degree of crystallinity of neat and nanoclay-infused biopol

	Crystallization temperature (°C)	Degree of crystallinity (%)	Degree of crystallinity change (%)	Melting temperature (°C)
Neat biopol	100.57	44.36	0	155
2% Nanoclay-biopol	99.77	47.46	6.98	154
3% Nanoclay-biopol	98.66	47.47	7.00	153
4% Nanoclay-biopol	98.47	47.67	7.46	153

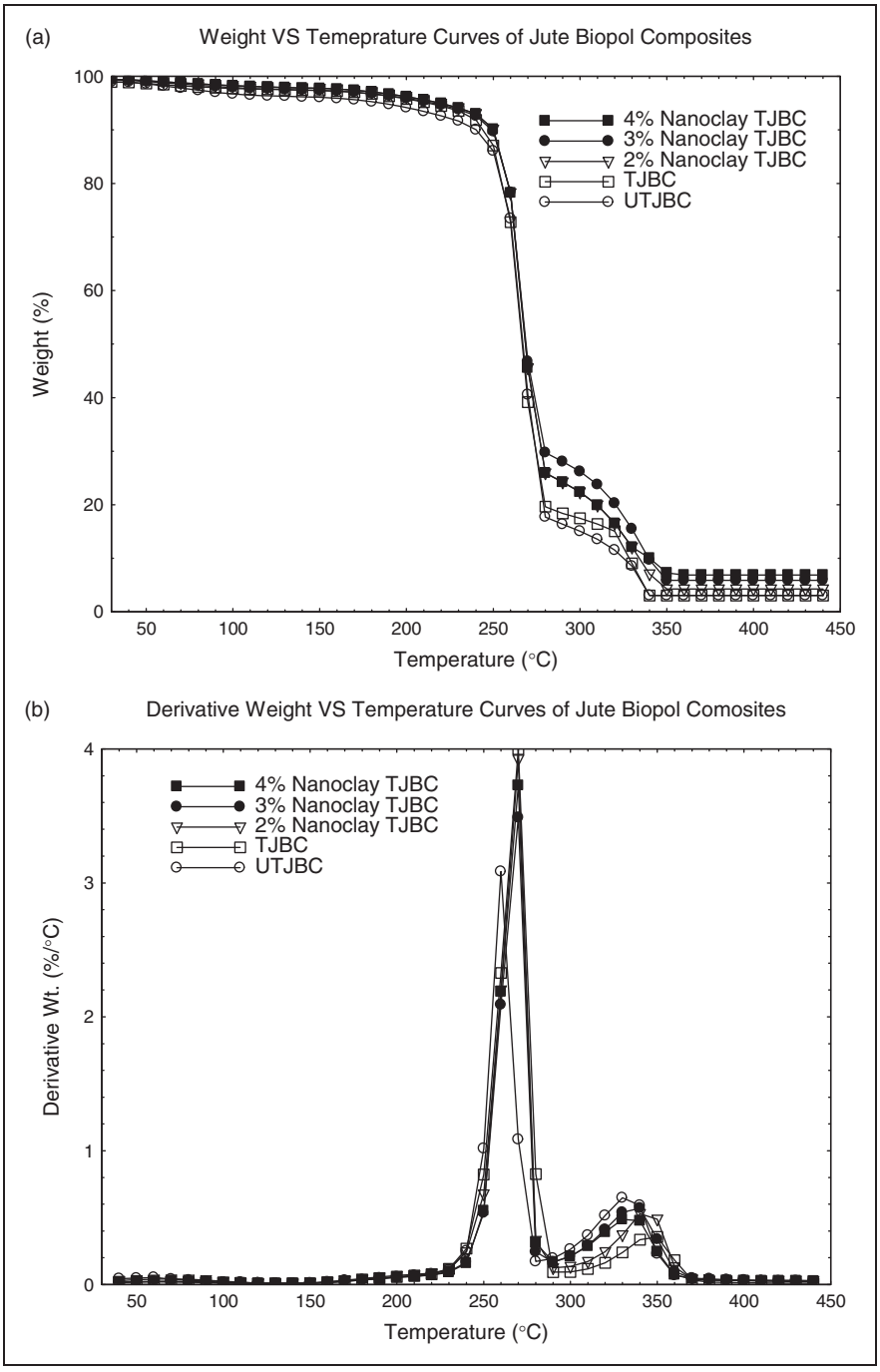

Figure 6. (a) Percentage weight loss and (b) derivative weight loss of jute–biopol composites with temperature.

the interaction of nanoclays' layers with PHBV chains, most of the nanoclays' layers restricted the motion of the PHBV chains. The restricted PHBV chains might not crystallize and hence, the crystallizable PHBV chains decreased. Therefore, the crystallization rate increased, whereas the relative degree of crystallinity decreased with increasing amount of nanoclays in the PHBV–nanoclay nanocomposites.[31]

Composite characterization

The fiber volume fraction determined using the composite mixing formula was found to be around 27%. This result was verified by performing the TGA. During TGA, all biopols were removed at 270°C and the remaining fiber and nanoparticles weight fractions were found to be 30%. The fiber volume calculation

using these weight fractions resulted in almost the same result as it was obtained from the mixing formula.

Decomposition temperatures of jute fibers and neat biopol are about 323°C and 265°C, respectively. Thermal degradation of biocomposites is a cumulative phenomenon of matrix and fiber.[44] Composites start to degrade around 270°C. Figure 6(a) shows that the nanoclay has no significant effect on the decomposition temperature. TJBC with nanoclay showed about 5% higher decomposition temperature compared to UTJBC (Figure 6(b)). Untreated fibers may contain some volatile materials, which may lead to decomposition at a lower temperature. Nanoclay-infused composites had a higher amount of residue, indicating that nanoclay did not degrade at 450°C and its weight is added with the residue of the fiber and matrix. Two distinct decomposition temperature regions were observed in these composites: first region for the matrix and second one for the fiber.

Thermal stability is critical for a material in many applications. Poor dimensional stability causes deformation during service. TMA was performed to find the thermal stability of these composites. Figure 7 and Table 3 show the data from CTE measurements of jute–biopol composites. Chemically treated jute–biopol composite has a lower CTE (212.4 μm/m°C) compared to untreated jute–biopol composite (266.8 μm/m°C). The change in dimension with temperature depends on the macromolecular activity and interaction between fiber and matrix.[45] Chemical modification resulted in a better adhesion and lower dimensional change with the temperature. Nanoclay-infused composites showed lower CTE than conventional composites. Nanoclay acts as a nucleating agent in a polymeric composite and retards the expansion of the polymer molecules when temperature increases. This results in a higher degree of crystallinity and higher dimensional stability. As the percentage of nanoclay increases, the CTE decreases, as given in Table 3.

DMA was performed to study the response of stiffness of the jute–biopol composites as a function of temperature. From DMA tests (Figure 8(a)), it was

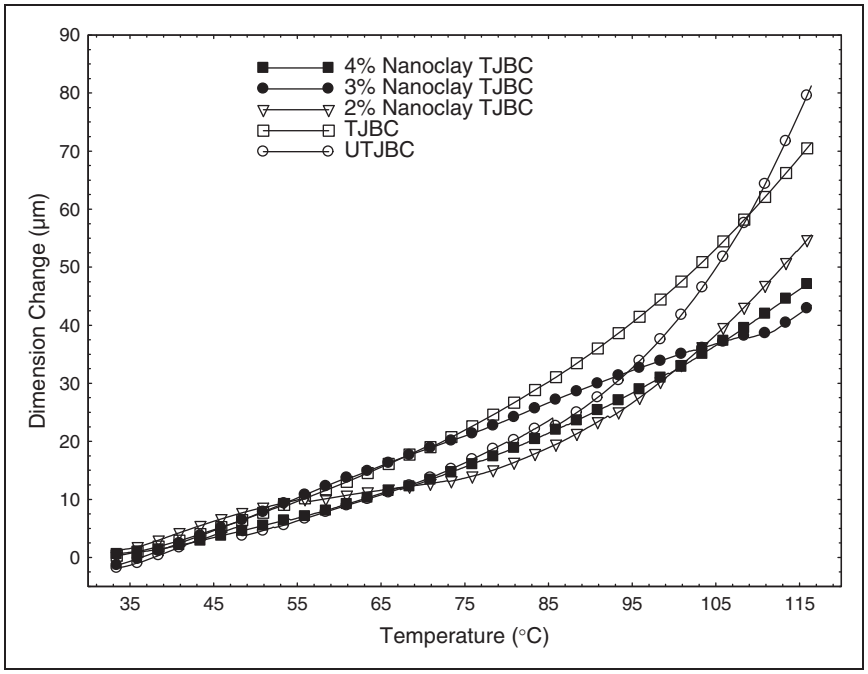

Figure 7. Dimension change vs. temperature curves of jute–biopol composites.

Table 3. Effect of surface treatment and nanoclay on the CTE of jute–biopol composites

	UTJBC	TJBC	2% Nanoclay TJBC	3% Nanoclay TJBC	4% Nanoclay TJBC
CTE (μm/m°C)	266.8 ± 6.4	212.4 ± 6.7	173.0 ± 4.5	164.20 ± 5.7	146.8 ± 4.8
Change in CTE (%)	0	19.6	35.1	38.45	44.9

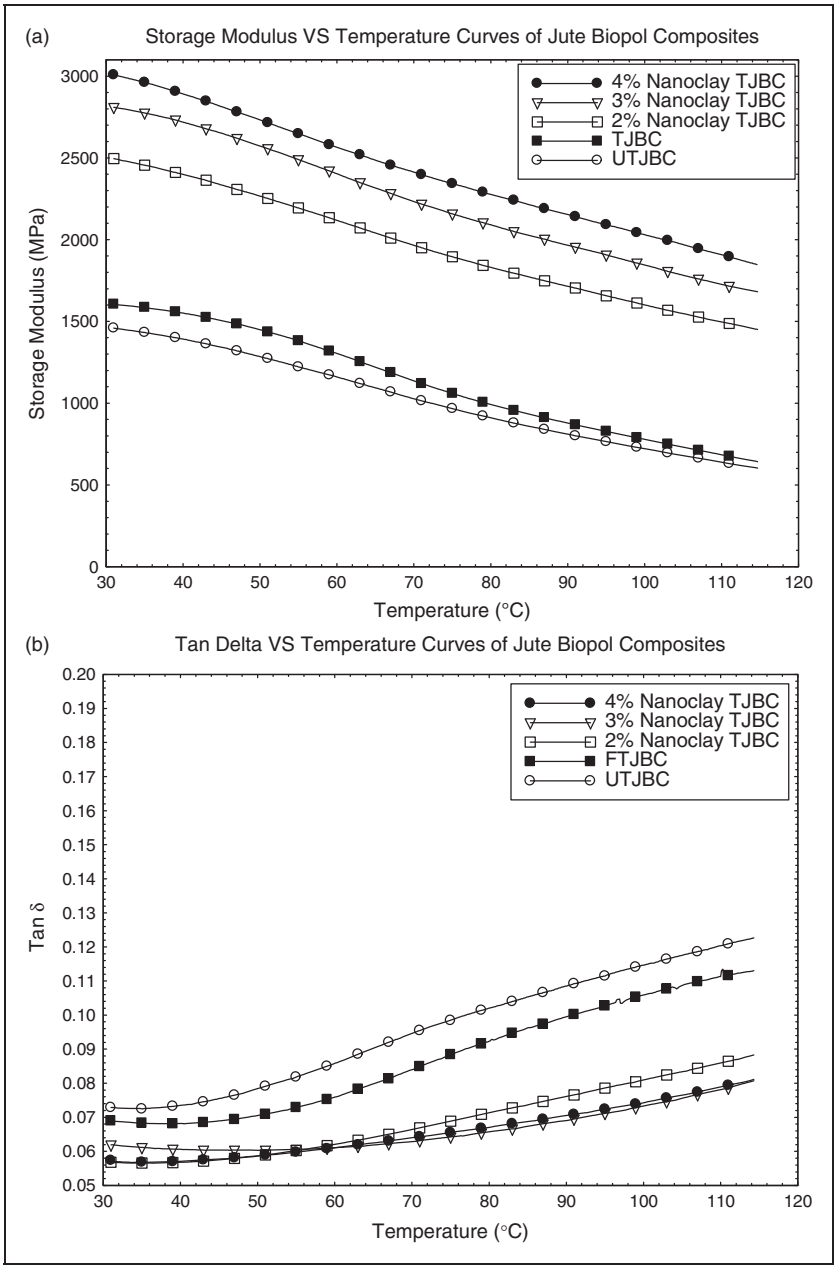

Figure 8. (a) Storage modulus and (b) tan δ of jute–biopol composites.

observed that storage modulus was the highest at room temperature and linearly decreased with increasing temperature. Storage modulus (1605 MPa) was higher in TJBC compared to UTJBC (1467 MPa). This may be attributed to the better interfacial bonding between fiber and matrix after the chemical treatment. The storage modulus values of jute–biopol samples with 2%, 3%, and 4% nanoclay were 2550, 2900, and 3050 MPa at 30°C, respectively. Higher storage modulus with increasing nanoclay content is an indication of higher degree of crystallinity and stiffness of the composites. On the other hand, optimal loading, uniform dispersion, and morphology of nanoparticles in matrix are the key parameters to promote better nanoparticle–matrix interface properties to reach an efficient load transfer between the two constituents of the nanocomposite.[46,47] It is expected that our solution intercalation technique was efficient enough to intercalate or exfoliate up to 4 wt% nanoclay uniformly throughout the PHBV. The main cause of intercalation or exfoliation was probably attributed to the hydrogen bonding interaction between PHBV and hydroxyl group in the gallery of nanoclay. The presence of aliphatic chains in the galleries altered the original nanoclay surface from

hydrophilicity to organophilicity. The adhesion between clay and PHBV matrix was improved. Thus, PHBV/nanoclay nanocomposites with high dispersion were produced.[31] Highly dispersed 4 wt% nanoclays in the PHBV matrices confined the PHBV chains and hindered the crystallization of the PHBV chains[48] and resulted in the stiffened matrix. Thus, evenly distributed stiff nanoclay-loaded all jute–biopol composites always showed better storage modulus than that of the composite without nanoclay.[49] This is attributed to the stiffened matrix of the composites. The interfacial area between the matrix and nanoclays was increased because of the high aspect ratio and uniform dispersion of the nanoclays, which in turn facilitated a better interaction between the treated-fiber and nanoclay-loaded matrix and ultimately improved the strength and stiffness compromising with the strain of the composites.[21] The nanoparticles also act as reinforcing element and bear the load in the composite material system.[50] When load is applied to the composite structures, the matrix starts to crack first and stress is then transferred from the lower modulus matrix to the stiffer nanoclays to the long fiber by bridging effect and ultimately the composites' properties are enhanced.[51] Moreover, dispersed nanoparticles act as mechanical interlocking between the fiber and matrix which creates a high friction coefficient, and resist the crack propagation in the composites during loading.[51] Thus, improved strength and stiffness result in the nanoclay-loaded jute fiber-reinforced biopol composites.

A small bump at around 50°C was observed in the samples without nanoclay. It indicates the cold crystallization temperature region. During the heating cycle, the specimen enters the cold crystallization region where crystallinity increases and the rate of decrease of storage modulus (E') decreases.[39] Lower cold crystallization temperature (about 40–45°C) was found in the samples with nanoclay, due to the clay's action as a nucleating agent in polymeric composites. Tangent delta (tan δ) as a function of temperature is illustrated in Figure 8(b). It provides the account of energy dissipated as heat during dynamic testing.[52] As the stiffness increases, tan δ value decreases, reflecting reduced energy losses. With increasing temperature, energy losses increase. Hence, the value of tan δ increases. Nanoclay infusion into the biocomposites decreased the tan δ value, indicating a higher degree of crystallinity. Crystalline structure reduces the loss modulus and increases the storage modulus. Loss modulus is related to the molecular chain movement of the polymer.

The ILSS of jute–biopol composites is shown in Figure 9. Interlaminar shear strength depends mainly on the matrix properties and fiber–matrix interfacial strength rather than the fiber properties. ILSS can be enhanced by increasing the matrix tensile strength and matrix volume fraction.[53] Chemically treated jute fiber-reinforced composites showed about 20% higher ILSS compared to UTJBC. Nanoclay-infused samples also showed higher ILSS values compared to those of TJBC and UTJBC samples. Nanoclay may result in a better interaction between fiber and matrix and higher crystallinity of biopol. The maximum value of ILSS was observed in 4 wt.% nanoclay-infused TJBC and the average value 4.67 MPa. These values of ILSS are lower than those of most other synthetic composites. Petroleum-based resins have higher ILSS values due to better interaction between fibers and matrix.[12,19] It has been reported that ILSS values of PP-based glass fiber composites[54,55] are about the same as observed in our study. Thus, it appears that biopol and PP behave in a similar fashion in a composite structure.

The fracture surfaces of ILSS-tested samples are shown in Figure 10. Smooth interlaminar debonding was observed in the UTJBC. The TJBC and nanoclay-infused TJBC showed better interfacial bonding. Nanoclay-infused TJBC composites showed fiber–matrix breakage followed by non-linear interlaminar delamination. Surface treatment results in better mechanical interlocking and interfacial bonding between the fiber and matrix. Nanoparticles also help in better interfacial bonding for their larger surface area and resist the crack propagation in the fiber-reinforced polymeric composites.[51]

Conclusions

The jute fibers were chemically treated to produce jute-based biocomposites. Nanoclay was infused into the biopol using solution intercalation techniques and thin films were prepared using compression molding machine. Jute–biopol composites were produced by stacking prepared biopol films with/without nanoclay and treated/untreated fibers in a sandwich construction using the compression molding process. The significant results obtained from the investigations are given below:

a. Surface treatments resulted in the removal of pectin, hemicellulose, and other non-cellulosic substances from the fibers and hence, a higher percentage of cellulose in the treated fibers. Rougher as well as increased surface areas were observed in treated fibers that are important for proper fiber wetting and better bonding with matrix. Surface-modified fibers showed a better decomposition temperature and tensile properties due to the presence of higher percentage of crystalline cellulose.
b. Biopol is semi-crystalline in nature. The nanoclay acted as a nucleating agent in the biopol. Thus, nanoclay-infused biopol showed a higher degree of crystallinity compared to the neat biopol.

c. Treated jute–biopol composites showed a better decomposition temperature, storage modulus, loss modulus, CTE, and ILSS compared to untreated jute–biopol composites due to better interaction between the fiber and matrix.
d. Nanophased jute–biopol composites showed better decomposition temperature, storage modulus, loss modulus, CTE, and ILSS compared to conventional untreated and treated jute–biopol composites. Properties of the jute-based biocomposites were observed to increase with increasing percentage of nanoclay. The 4 wt% nanoclay-infused composites showed better results compared to those with 2 wt% and 3 wt% nanoclays, which was further demonstrated by OM studies.

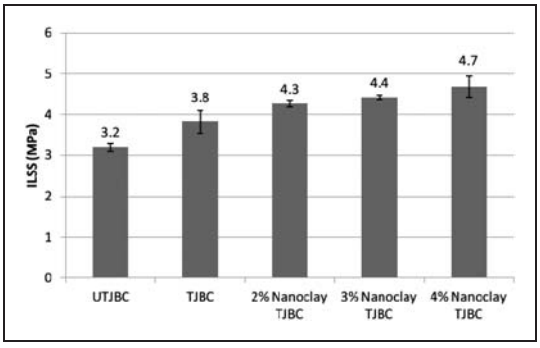

Figure 9. ILSS of jute–biopol composites.

Funding

This research study received financial support from NSF-EPSCoR (grant no. EPS-0814103) and NSF-RISE (grant no. HRD-0833158).

References

1. Doan T, Gao S and Mader E. Jute/polypropylene composites. I. Effect of matrix modification. *Compos Sci Technol* 2006; 66: 952–963.
2. Zini E, Focarete ML, Noda I and Scandola M. Biocomposite of bacterial poly (3- hydroxybutyrate-co-3-hydroxyhexanoate) reinforced with vegetable fibers. *Compos Sci Technol* 2007; 67: 2085–2094.
3. Mantia FP and Morreale M. Green composites: a brief review. *Composites Part A* 2011; 42(6): 579–588.
4. Sandler J, Werner P, Shaffer MSP, Denchuk V, Altstadt V and Windle AH. Carbon nanofibers reinforced poly (ether ether ketone) composites. *Composites Part A* 2002; 33: 1033–1039.

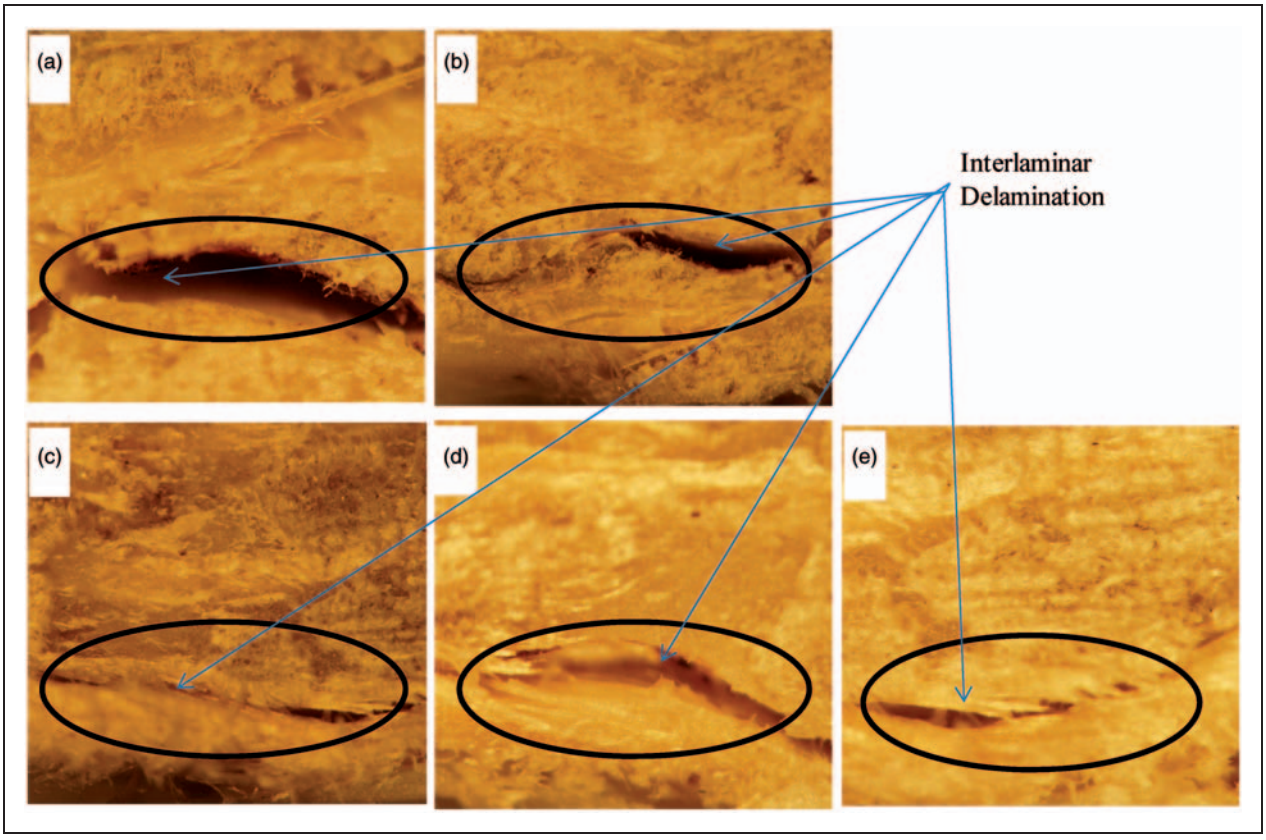

Figure 10. Optical micrographs of the fracture surfaces of ILSS-tested specimens.

5. Zini E, Bairado M and Scandola M. Biodegradable polyesters reinforced with surface-modified vegetable fibers. *Macromol Biosci* 2004; 4: 286–295.
6. Xie Y, Kohls D, Noda I, Schaefer D and Akpalu Y. Poly (3-hydroxybutyrate-co-3-hydroxyhexanoate) nanocomposites with optimal mechanical properties. *Polymer* 2009; 50: 4656–4670.
7. Sudesh K, Abe H and Doi Y. Synthesis, structure and properties of poly-hydroxyalkonates: biological polyesters. *Prog Polym Sci* 2000; 25: 1503–1555.
8. Barkoula NM, Garkhail SK and Peijs T. Biodegradable composites based on flax/polyhydroxybutyrate and its copolymer with hydroxyvalerate. *Ind Crops Prod* 2010; 1: 34–42.
9. Jiang L, Morelius E, Zhang J, Wolcott M and Holbery J. Study of the poly(3-hydroxybutyrate-co-3-hydroxyvalerate)/cellulose nanowhisker composites prepared by solution casting and melt processing. *J Compos Mater* 2008; 42: 2629–2645.
10. Singh S, Mohanty AK, Sugie T, Takai Y and Hamada H. Renewable resource based biocomposites from natural fiber and polyhydroxybutyrate-co-valerate (PHBV) bioplastic. *Composites Part A* 2008; 39: 875–886.
11. John MJ and Thomas S. Review bio-fibers and biocomposites. *Carbohydr Polym* 2008; 71: 343–364.
12. Gowda TM, Naidu ACB and Chhaya R. Some mechanical properties of untreated jute fabric reinforced polyester composites. *Composites Part A* 1999; 30: 277–284.
13. Corrales F, Vilaseca F, Llop M, Girones J, Mendez JA and Mutje P. Chemical modification of jute fibers for the production of green-composites. *J Hazard Mater* 2007; 144: 730–735.
14. Wong S, Shanks R and Hodzic A. Interfacial improvements in poly(3-hydroxybutyrate)-flax fibre composites with hydrogen bonding additives. *Compos Sci Technol* 2004; 64(9): 1321–1330.
15. Pejic BM, Kostic MM, Skundric PD and Praskalo JZ. The effects of hemicelluloses and lignin removal of on water uptake behavior of hemp fibers. *Bioresour Technol* 2008; 99: 2686–2699.
16. Ray D and Sarkar BK. Characterization of alkali treated jute fibers for physical and mechanical properties. *J Appl Polym Sci* 2001; 80: 1013–1020.
17. Acha BA, Marcovich NE and Reboredo MM. Physical and mechanical characterization of jute fabric composites. *J Appl Polym Sci* 2005; 98(2): 639–650.
18. Bledzki AK, Mamun AA and Faruk O. Abaca fibre reinforced PP composites and comparison with jute and flax fibre PP composites. *Express Polym Lett* 2007; 1(11): 755–762.
19. Hwang B, Kim B, Lee J, Byun J and Park J. Physical parameters and mechanical properties improvement for jute fiber/polypropylene composites by maleic anhydride coupler. In: *16th International Conference on Composite Materials*, Kyoto, Japan, 8–13 July 2007, pp. 1–7.
20. Hong CK, Hwang I, Kim N, Park DH, Hwang BH and Nah C. Mechanical properties of silanized jute-polypropylene composites. *J Ind Eng Chem* 2008; 14: 71–76.
21. Bruzaud S and Bourmaud A. Thermal degradation and (nano) mechanical behavior of layered silicate reinforced poly (3-hydroxybutyrate-co-3-hydroxyvalerate) nanocomposites. *Polym Test* 2007; 26: 652–659.
22. Huang G and Netravali A. Characterization of flax fiber reinforced soy protein resin based green composites modified with nano-clay particles. *Compos Sci Technol* 2005; 67: 2005–2014.
23. Mohanty AK, Wibowo A, Misra M and Drzal LT. Effect of process engineering on the performance of natural fiber reinforced cellulose acetate biocomposites. *Composites Part A* 2004; 35: 363–370.
24. Haque MM, Hasan M, Islam MS and Ali ME. Physico-mechanical properties of chemically treated palm and coir fiber reinforced polypropylene composites. *Bioresour Technol* 2009; 100: 4903–4906.
25. Fan Z, Santare M and Advani S. Interlaminar shear strength of glass fiber reinforced epoxy composites enhanced with multi-walled carbon nanotubes. *Composites Part A* 2008; 39: 540–554.
26. Brydson J. *Plastics materials*, 7th edn. Woburn, MA: Butterworth-Heinemann, 1999.
27. Sinha S and Rout SK. Influence of fiber-surface treatment on structural, thermal and mechanical properties of jute fiber and its composite. *Bull Mater Sci* 2009; 32: 65–76.
28. Mwaikambo LY and Ansell MP. Chemical modification of hemp, sisal, jute, and kapok fibres by alkalization. *J Appl Polym Sci* 2009; 84: 2222–2234.
29. Hossain MK, Dewan MW, Hosur M and Jeelani S. Mechanical performances of surface modified jute fiber reinforced biopol nanophased green composites. *Composites Part B* 2011; 42(6): 1701–1707.
30. Vilaseca F, Mendez JA, Pelach A, Llop M, Canigueral N, Girones J, et al. Composite materials derived from biodegradable starch polymer and jute strands. *Process Biochem* 2007; 42: 329–334.
31. Wang S, Song C, Chen G, Guo T, Liu J, Zhang B, et al. Characterization and biodegradation properties of poly(3-hydroxybutyrate-co-3-hydroxyvalerate) organophilic montmorillonite (PHBV/OMMT) nanocomposite. *Polym Degrad Stab* 2005; 87: 69–76.
32. Liu Y, Tang R, Yu J and Wang K. Investigation of interfacial structure of coupling agent treated fillers by Fourier transform infrared spectroscopy and attenuated total reflection-FTIR spectroscopy. *Polym Compos* 2002; 23(1): 28–33.
33. Xie YP, Noda I and Akpalu YA. Influence of cooling rate on the thermal behavior and solid-state morphologies of polyhydroxyalkanoates. *J Appl Polym Sci* 2008; 109(4): 2259–2268.
34. ASTM D 4065-01. *Standard practice for plastics: Dynamic mechanical properties: Determination and report of procedures. Annual book of ASTM standards*. West Conshohocken, PA: American Society for Testing and Materials, 2002.
35. Ganan P, Zulunga R, Restrepo A, Labidi J and Mondragon I. Plantain fibre bundles isolated from colombian agro-industrial restudies. *Bioresour Technol* 2008; 99: 486–491.
36. Saha P, Manna S, Chowdhury SR, Sen R, Roy D and Adhikari B. Enhancement of tensile strength of

lignocellulosic jute fibers by alkali-steam treatment. *Bioresour Technol* 2010; 101: 3182–3187.
37. Sui G, Fuqua MA, Ulven CA and Zhong WA. A plant fibre reinforced polymer composite prepared by a twin-screw extruder. *Bioresour Technol* 2009; 100: 1246–1251.
38. Sinha E and Rout SK. Influence of fiber-surface treatment on structural, thermal and mechanical properties of jute. *J Mater Sci* 2008; 43: 2590–2601.
39. Khan MA, Ganster J and Fink HP. Hybrid composites of jute and man-made cellulose fibers with polypropylene by injection molding. *Composites Part A* 2009; 40: 846–851.
40. Wong S, Shanks R and Hodzic A. Interfacial improvements in poly(3-hydroxybutyrate)-flax fibre composites with hydrogen bonding additives. *Compos Sci Technol* 2004; 64: 1321–1330.
41. Velde KV and Baetens E. Thermal and mechanical properties of flax fibres as potential composite reinforcement. *Macromol Mater Eng* 2001; 286: 342–349.
42. Park JM, Quang ST, Hwang BS and Devries KL. Interfacial evaluation of modified jute and hemp fibers/polypropylene (PP)-maleic anhydride polypropylene copolymers (PP-MAPP) composites using micromechanical technique and nondestructive acoustic emission. *Compos Sci Technol* 2006; 66: 2686–2699.
43. Renstad R, Karlsson S, Albertsson AC, Werner PE and Westdahl M. Influence of processing parameters on the mass crystallinity of poly(3-hydroxybutyrate-co-3-hydroxyvalerate). *Polym Int* 1997; 43: 201–209.
44. Martins MA, Kiyohara PK and Joekes I. Scanning electron microscopy study of raw and chemically modified sisal fibers. *J Appl Polym Sci* 2004; 94: 2333–2340.
45. Sui G, Jana S, Salehi-khojin A, Neema S, Zhong WH, Chen H, et al. Thermal and mechanical properties of epoxy composites reinforced by a natural hydrophobic sand. *J Appl Polym Sci* 2008; 109: 247–255.
46. Zhou Y, Pervin F, Jeelani S and Mallick PK. Improvement in mechanical properties of carbon fabric–epoxy composite using carbon nanofibers. *J Mater Process Technol* 2008; 198(1–3): 445–453.
47. Prolongo SG, Burón M, Gude MR, Chaos-Morán R, Campo M and Ureña A. Effects of dispersion techniques of carbon nanofibers on the thermo-physical properties of epoxy nanocomposites. *Compos Sci Technol* 2008; 68(13): 2722–2730.
48. Ma J, Zhang S, Qi Z, Li G and Hu Y. Crystallization behaviors of polypropylene/montmorillonite nanocomposites. *J Appl Polym Sci* 2002; 83: 1978–1985.
49. Krikorian V, Kurian M, Galvin ME, Nowak AP, Deming TJ and Pochan DJ. Polypeptide-based nanocomposite: structure and properties of poly(L-lysine)/Na^+-montmorillonite. *J Appl Polym Sci* 2002; 40: 2579–2586.
50. Jawahar P, Gnanamoorthy R and Balasubramanian M. Tribological behavior of clay-thermoset polyester nanocomposites. *Wear* 2006; 261: 835–840.
51. Hossain MK, Hossain ME, Hosur M and Jeelani S. Flexural and compression response of woven E-glass/polyester-CNF nanophased composites. *Composites Part A* 2011; 42(11): 1774–1782.
52. Menard KP. *Time-temperature scans: Transitions in polymers, dynamic mechanical analysis: A practical introduction*. Boca Raton, FL: CRC Press LLC, 1999.
53. Ahmed KS and Vijayarangan S. Tensile, flexural and interlaminar shear properties of woven jute and jute-glass fabric reinforced polyester composites. *J Mater Process Technol* 2008; 207: 330–335.
54. Hoecker F and Karger-Kocsis J. Effects of crystallinity and supermolecular formations on the interfacial shear strength and adhesion in GF/PP composites. *Polym Bull* 1993; 31: 707–714.
55. Rausch J, Zhuang RC and Mader E. Systematically varied interfaces of continuously reinforced glass fibre/polypropylene composites: comparative evaluation of relevant interfacial aspects. *Express Polym Lett* 2010; 4(9): 576–588.